Integrated analysis of multiple transcriptomic data identifies ST8SIA6-AS1 and LINC01093 as potential biomarkers in HBV-associated liver cancer

JIANHUA XUE[1*], HUI ZHAO[1*], YIFEI FU[1], XU LIU[1] and XIANGXIANG WU[2]

[1]Department of Infectious Diseases, Hospital for Infectious Diseases of Pudong District, Shanghai 201318; [2]Department of Traditional Chinese Medicine, Yueyang Hospital of Integrated Traditional Chinese and Western Medicine, Shanghai University of Traditional Chinese Medicine, Shanghai 200437, P.R. China

Received July 26, 2022; Accepted December 2, 2022

DOI: 10.3892/ol.2023.13771

Abstract. The mechanisms of long-non-coding RNAs (lncRNAs) in hepatitis B virus (HBV) infection-associated liver cancer remain largely unclear. Therefore, the aim of the present study was to investigate the regulatory mechanisms of lncRNAs in this disease. HBV-liver cancer related transcriptome expression profile data (GSE121248 and GSE55092) from the Gene Expression Omnibus database and survival prognosis information from The Cancer Genome Atlas (TCGA) database were obtained for analysis. The limma package was used to identify the overlapped differentially expressed RNAs (DERs), including DElncRNAs and DEmRNAs, in the GSE121248 and GSE55092 datasets. The screened optimized lncRNA signatures were used to develop a nomogram model based on the GSE121248 dataset, which was validated using the GSE55092 and TCGA datasets. A competitive endogenous RNA (ceRNA) network was constructed based on the screened prognosis-associated lncRNA signatures from TCGA dataset. In addition, the levels of specific lncRNAs were evaluated in HBV-infected human liver cancer tissues and cells, and Cell Counting Kit-8, ELISA and Transwell assays were performed to evaluate the effects of the lncRNAs in HBV-expressing liver cancer cells. A total of 535 overlapped DERs, including 30 DElncRNAs and 505 DEmRNAs, were identified in the GSE121248 and GSE55092 datasets. An optimized DElncRNA signature comprising 10 lncRNAs was used to establish a nomogram. ST8SIA6-AS1 and LINC01093 were identified as lncRNAs associated with HBV-liver cancer prognosis in TCGA dataset, and were applied to construct a ceRNA network. Reverse transcription-quantitative PCR analysis showed that ST8SIA6-AS1 was upregulated and LINC01093 was downregulated in HBV-infected human liver cancer tissues and HBV-expressing liver cancer cells compared with non-HBV-infected controls. ST8SIA6-AS1 knockdown and LINC01093 overexpression independently reduced the number of copies of HBV DNA, the levels of hepatitis B surface antigen and hepatitis B e antigen, as well as cell proliferation, migration and invasion. In summary, the present study identified ST8SIA6-AS1 and LINC01093 as two potential biomarkers that may be effective therapeutic targets for HBV-associated liver cancer.

Correspondence to: Dr Xiangxiang Wu, Department of Traditional Chinese Medicine, Yueyang Hospital of Integrated Traditional Chinese and Western Medicine, Shanghai University of Traditional Chinese Medicine, 110 Ganhe Road, Hongkou, Shanghai 200437, P.R. China
E-mail: wi_xiangxiang0201@126.com

*Contributed equally

Key words: HBV-associated liver cancer, transcriptomic data, bioinformatics analysis, nomogram, ceRNA

Introduction

Liver cancer is one of the most common types of malignant tumor and a leading cause of cancer-associated deaths worldwide (1). Hepatitis B virus (HBV) infection has been demonstrated to be an important risk factor for high-risk liver cancer (2). Multiple studies have reported that HBV contributes to the proliferation and metastasis of liver cells, playing a crucial role in the high recurrence and mortality of liver cancer (3-5). Despite improvements that have been made in surgical resection and transplantation, the prognosis of patients with liver cancer remains unsatisfactory with a 5-year survival rate of <50% (6,7). Therefore, exploring the molecular mechanism underlying the pathogenesis of HBV-associated liver cancer has important clinical significance.

Non-coding RNAs (ncRNAs) are divided into small ncRNAs with 18-200 nucleotides, known as microRNAs (miRNAs), and long ncRNAs (lncRNAs) of between 200 nucleotides and 100 kb, which represent the majority of human genome transcripts (8). Numerous studies have documented the crucial roles of lncRNAs as regulators of viral replication or the antiviral response in the pathogenesis and progression of HBV-induced liver cancer (9,10). For instance, HBV X protein-related long ncRNA MALAT1 has been shown to promote cell metastasis via the upregulation of latent

transforming growth factor β binding protein 3 expression in liver cancer (11). In another study, lncRNA MAPKAPK5_AS1 was found to be upregulated in HBV-associated liver cancer tissues, and facilitated the proliferation and G1/S transition in HBV-positive liver cancer cells (12). Conversely, Deng *et al* (13) found that another lncRNA, F11-AS1, suppressed HBV-associated liver cancer progression via interference with cellular physiology. Additionally, well-explored lncRNAs, including DBH antisense RNA 1 (14), HOX transcript antisense intergenic RNA (15) and X inactive specific transcript (16) have been reported to be potential prognostic biomarkers for patients with HBV-associated liver cancer. Nevertheless, most of these studies focused on a single lncRNA and comprehensive analysis of the lncRNA signature of HBV-associated liver cancer is relatively limited (17).

In the present study, the transcriptome expression level data of samples from patients with liver cancer and HBV infection were comprehensively analyzed on multiple platforms. Based on the lncRNAs and genes identified to be associated with HBV-related liver cancer, different optimization algorithms were used to further screen the optimized lncRNA signatures. Following the construction of a competing endogenous RNA (ceRNA) regulatory network, functional experiments were performed to investigate the biological role of characteristic lncRNAs. These experiments were performed with the aim of identifying novel therapeutic targets for the diagnosis and treatment of patients with HBV-associated liver cancer.

Materials and methods

Data collection. Transcriptome expression profile data for HBV-associated liver cancer were searched for in the Gene Expression Omnibus (GEO) database (http://www.ncbi.nlm.nih.gov/geo) with the keywords 'hepatitis' and 'liver cancer'. The final date covered by the search was May 16, 2022, The following inclusion criteria were used: i) Transcriptome expression profile data; ii) subjects were skin solid tissue samples from patients with liver cancer; iii) included hepatitis virus infection data; iv) contained normal control specimens; v) sample size >100; vi) the detection platform was capable of annotating a large number of lncRNAs. As a result, two sets of transcriptome expression profile data obtained using the GPL570 Affymetrix Human Genome U133 Plus 2.0 Array platform were screened as follows: GSE121248, which contains 70 HBV-liver cancer samples and 37 control samples (18) as the training dataset, and GSE55092, which contains 39 HBV-liver cancer samples and 81 control samples (19) as the validation dataset. In addition, the Ensembl genome browser 96 database (http://asia.ensembl.org/index.html) was used to download detailed platform annotation information, including probes, gene symbols and RNA types. The expression levels of corresponding lncRNAs and mRNAs were obtained by reannotating the detection probes downloaded from these two datasets.

In addition, transcriptome expression profile data for patients with liver cancer were collected from The Cancer Genome Atlas (TCGA) database (https://portal.gdc.cancer.gov/) based on the Illumina HiSeq 2000 RNA Sequencing platform as an independent validation dataset. After the removal of samples without viral hepatitis serology information, 60 HBV-liver cancer samples with survival prognosis information and 46 control samples were obtained.

Screening of overlapped differentially expressed RNAs (DERs). The limma package of R3.6.1 version 3.34.7 (20) was utilized to screen the DERs, including DElncRNAs and DEmRNAs, between the HBV-liver cancer and normal control groups in GSE121248 and GSE55092. The cutoff value for screening was $|\log_2$ fold change (FC)$|>1.0$ and FDR (false discovery rate) <0.05. Then, the selected DERs were used to draw a volcano plot and heatmap. A Venn diagram was created to display the DERs that were present in both datasets. Using DAVID version 6.8 (21,22) (https://david.ncifcrf.gov/), the DEmRNAs common to both datasets were subjected to Gene Ontology (GO) function and Kyoto Encyclopedia of Genes and Genomes (KEGG) pathway enrichment analysis with FDR <0.05 as the cutoff criterion.

Construction and validation of a nomogram. The optimized lncRNA signatures were first screened in the GSE121248 dataset using three types of optimization algorithms, including recursive feature elimination (RFE) (23), least absolute shrinkage and selection operator (LASSO) (24) and random forest (RF) (25). By comparing these results, the DElncRNAs common to all three analyses were used as the final optimized lncRNA signatures. A concise nomogram for predicting the survival of patients with HBV-liver cancer was established in the training dataset using the rms package version 5.1-2 in R3.6.1 language (26). Then, the R3.6.1 language rmda package version 1.6 (https://cran.r-project.org/web/packages/rmda/index.html) was used to perform decision curve analysis on individual optimized lncRNA or combined optimized lncRNA signatures. Finally, the nomogram model constructed based on the previously screened optimized lncRNA signatures was verified as a diagnostic model in the validation dataset GSE55092 and TCGA independent validation dataset.

Prognostic performance of the HBV-associated lncRNA signature in liver cancer. The obtained optimized lncRNA signatures were subjected to univariate Cox regression analysis to screen the HBV prognosis-associated lncRNA signatures from TCGA dataset. The samples were divided into high and low expression groups according to their expression median levels. The association between different expression levels and survival prognosis was evaluated using the Kaplan-Meier curve method with log-rank test.

Construction of a ceRNA network based on the prognostic lncRNAs signature. According to the ceRNA hypothesis, a lncRNA-miRNA-mRNA ceRNA interaction network was constructed as follows: Liver cancer-associated miRNAs were mined from the miR2Disease version 2022 database (27). By searching the DIANA-LncBase v2 database (28), the validated relationships of the lncRNAs ST8SIA6-AS1 or LINC01093 with liver cancer-related miRNAs were obtained with MitScore >0.6 as the cutoff and the lncRNA-miRNA interactions were constructed. Then, the corresponding mRNA targets of the liver cancer-associated miRNAs were predicted by searching StarBase version 2.0 (29). Subsequently, the predicted mRNA targets of the liver cancer-associated miRNAs were combined

with the consistently expressed overlapping DEmRNAs to obtain the final miRNA-mRNA interactions. Finally, the lncRNA-miRNA-mRNA ceRNA network was constructed based on lncRNA-miRNA and miRNA-mRNA interactions and visualized using Cytoscape version 3.6.1 (30). To elucidate the functions of important lncRNAs, KEGG pathway enrichment analysis was performed on the DEmRNAs contained in the ceRNA network.

HBV-associated tissue samples. A total of 31 pairs of tumor tissues and adjacent liver tissues were obtained from patients with HBV-associated liver cancer (age range, 21-72 years; mean age, 42.5±7.8 years; 10 females and 21 males) at the Hospital for Infectious Diseases of Pudong District (Shanghai, China) between August 2020 and September 2021. Prior to tissue collection, each patient provided written informed consent for the use of their samples in scientific research. The obtained tissues were immediately snap-frozen in liquid nitrogen until further analysis. This study complied with the guidelines of the Declaration of Helsinki and was approved by the Ethics Committee of the Hospital for Infectious Diseases of Pudong District (approval no. IDP-2020PD; 2020.8.16).

Cell transfection and culture. The HepG2 human hepatoblastoma cell line and the HepG2.2.15 cell line, which was derived from HepG2 cells via the integration of the full-length HBV genome into the cellular genome, were purchased from American Type Culture Collection. The identification of the two cell lines was confirmed using short tandem repeat DNA profiling analysis. The cell lines were cultured in DMEM (Thermo Fisher Scientific, Inc.) with 10% FBS, 100 U/ml penicillin and 0.1% (w/v) streptomycin in a humidified incubator with 5% CO_2 at 37˚C. The small interfering (si)RNAs si-ST8SIA6-AS1 (5'-GCTCCTCCTTGCTCCAAAGAA-3') and si-negative control (si-NC; 5'-GCAGATCCTACCCGTCTCTAA-3') and the plasmids pcDNA3.1 and pcDNA3.1-LINC01093 were synthesized by Shanghai GenePharma Co., Ltd. These oligonucleotides or plasmids (50 μg) were transfected into HepG2.2.15 cells using Lipofectamine® 2000 (Invitrogen; Thermo Fisher Scientific, Inc.) at 37˚C for 48 h, and then harvested immediately for subsequent experiments.

Reverse transcription-quantitative PCR (RT-qPCR). Total RNA was isolated from tissues or cells using TRIzol® reagent (cat. no. 10296010; Invitrogen; Themo Fisher Scientific, Inc.). RT was performed using a PrimeScript RT reagent kit with gDNA Eraser (Takara Bio, Inc.) following the manufacturer's instructions. qPCR was carried out using SYBR® Premix Ex Taq II (Takara Bio, Inc.) with the following primer sequences: ST8SIA6-AS1 forward. 5'-TCCTGATTCAGTGGCATGGT-3' and reverse, 5'-AGGGTTTCTTCGGTCGTCAT-3'; LINC01093 forward, 5'-CTCTTGCAAACCATGGGCAC-3' and reverse, 5'-CATCTCCCAGTCGGGTTTCC-3'; GAPDH forward, 5'-GGTGAAGGTCGGAGTCAACG-3' and reverse, 5'-GCATCGCCCCACTTGATTTT-3'. The thermocycling conditions were 94˚C for 30 sec, followed by 40 cycles of 94˚C for 5 sec and 60˚C for 30 sec. Relative expression levels of target genes were calculated using the $2^{-\Delta\Delta Cq}$ method (31) with GAPDH as the reference gene.

HBV replication analysis. The HBV DNA was extracted from cell supernatants using a Column Viral DNAout kit (Tiandz, Inc.) according to the manufacturer's instructions. HBV DNA levels were determined by qPCR using QuantiFast SYBR® Green PCR Kit (Qiagen, Inc.) with the following primer sequences: Forward, 5'-GCCTCATTTTGCGGATCACC-3' and reverse, 5'-TGTCCCCATGCCTTTTCGAG-3'. Relative expression levels of target genes were calculated using the $2^{-\Delta\Delta Cq}$ method (31) with GAPDH as the reference gene.

Enzyme-linked immunosorbent assay (ELISA). In brief, the cell culture supernatants of HepG2.2.15 cells were centrifuged at 250 x g for 5 min at 4˚C and kept -20˚C until further analysis. Then, the viral protein hepatitis B surface antigen (HBsAg) and hepatitis B e antigen (HBeAg) in the culture supernatant were determined using corresponding ELISA kits (cat. nos. CSB-E10089h and CSB-E13557h, respectively; Cusabio Technology, LLC).

Cell Counting Kit-8 (CCK-8) assay. Cell proliferation capacity was assessed by performing a CCK-8 assay. Briefly, HepG2.2.15 cells at a density of 5,000 cells per well were seeded into 96-well plates and cultured overnight. At 0, 24, 48 and 72 h, 10 μl CCK-8 reagent (Dojindo Laboratories, Inc.) was separately added into each well. After incubation for another 2 h, the optical density (OD) of each well was measured at 450 nm using a microplate reader (Bio-Rad Laboratories, Inc.).

Migration and invasion assays. The *in vitro* migration assay was performed using Transwell chambers (pore size, 8.0 μm; Corning Costar). For invasion assays, the upper surface of the Transwell chamber was precoated with Matrigel for 2 h at 37˚C (Corning Costar) in advance, while for migration assays no coating was applied. Subsequently, ~$5x10^4$ HepG2.2.15 cells in serum-free medium were placed in the upper Transwell chamber, while the lower chamber was filled with complete medium. After 24 h incubation at 37˚C, the transferred cells on the lower chamber were fixed with 70% ethanol for 30 min and stained with 0.2% crystal violet for 15 min at room temperature. The stained cells were photographed and counted in five random fields under a light microscope (Olympus Corporation).

Statistical analysis. GraphPad Prism software (version 8.0; GraphPad Software, Inc.) was used to perform the statistical analysis of all quantitative data. The data were expressed as the mean ± standard deviation of three independent experiments. Differences between two groups were assessed using paired Student's t-tests for comparing tumor adjacent tissues and unpaired Student's t-tests for comparing two cell groups. Comparisons among three groups were performed using one-way ANOVA followed by Tukey post hoc tests. $P<0.05$ was considered to indicate a statistically significant result.

Results

Identification of DERs and functional enrichment analysis in patients with HBV-liver cancer. The differential analysis of HBV-liver cancer and control groups with a cutoff value of $|\log_2 FC|>1.0$ and FDR <0.05 yielded 1,183 DERs (Table SI) in GSE55092 (Fig. 1A and B) and 666 DERs in GSE121248

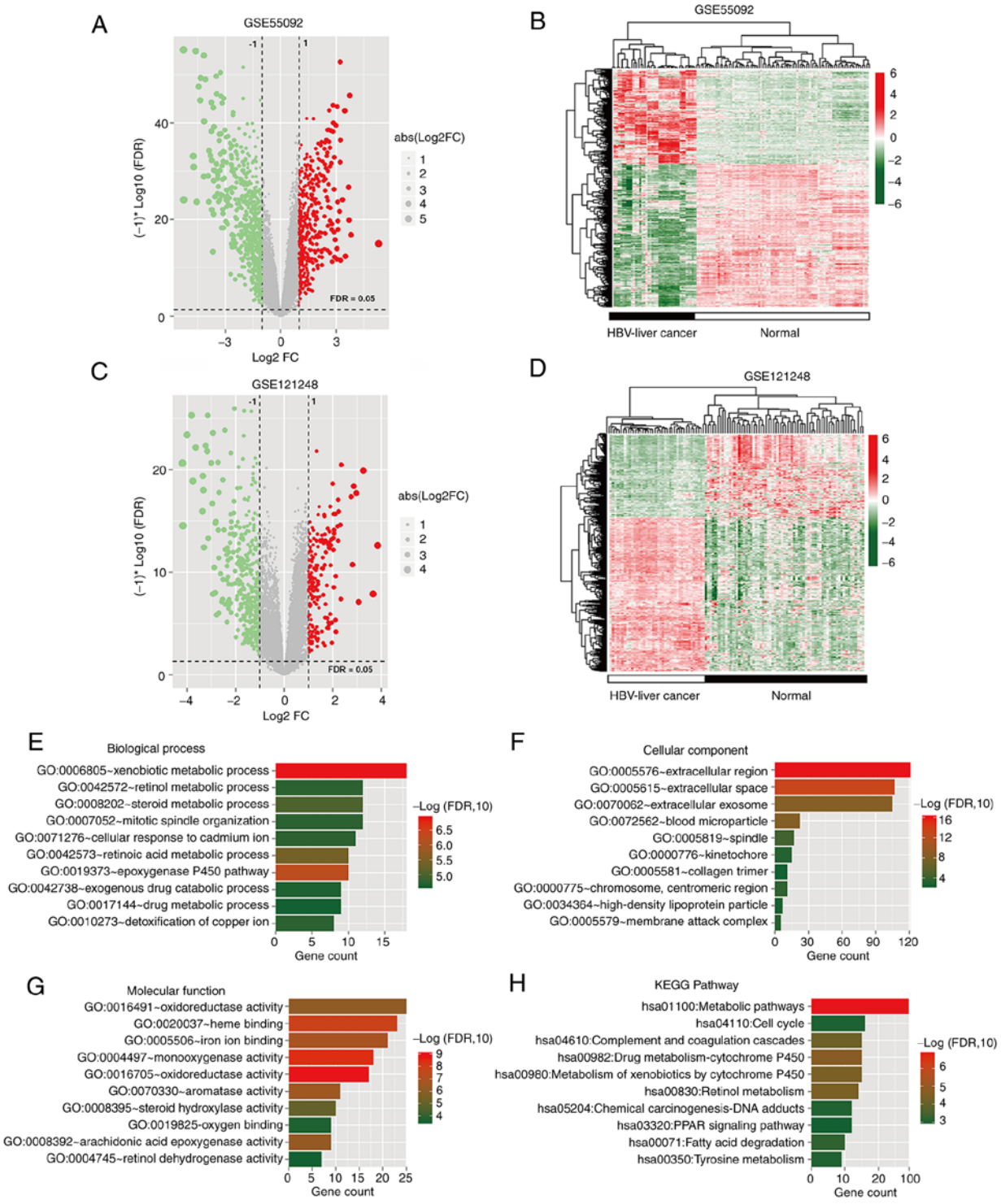

Figure 1. Identification of DERs and functional enrichment analysis in patients with HBV-liver cancer. (A) Volcano map and (B) heatmap presenting the differential expression of DERs between HBV-liver cancer and normal controls in the GSE55092 dataset. (C) Volcano map and (D) heatmap presenting the differential expression of DERs between HBV-liver cancer and normal controls in the GSE121248 dataset. (E) GO terms for the top 10 enriched biological processes. (F) GO terms for the top 10 enriched cellular components. (G) GO terms for the top 10 enriched molecular functions. (H) KEGG enrichment analysis showing the top 10 enriched pathways. DERs, differentially expressed RNAs; HBV, hepatitis B virus; GO, Gene Ontology; KEGG, Kyoto Encyclopedia of Genes and Genomes.

(Fig. 1C and D). A total of 535 DERs were identified to be common to both datasets (Table SII); Venn diagrams showing the overlap demonstrated that the DERs included 30 DElncRNAs, of which 14 were upregulated and 16 were downregulated, and 505 DEmRNAs of which 164 were upregulated and 341 were downregulated (Fig. S1). Subsequently, functional enrichment analysis was performed on the 505 overlapping DEmRNAs (Table SIII). The 505 DEmRNAs were significantly enriched in numerous GO terms, including 48 biological process (Fig. 1E), 18 cellular component (Fig. 1F) and 24 molecular function terms (Fig. 1G), as well as 19 KEGG signaling pathways (Fig. 1H), of which the top 10 terms are respectively displayed.

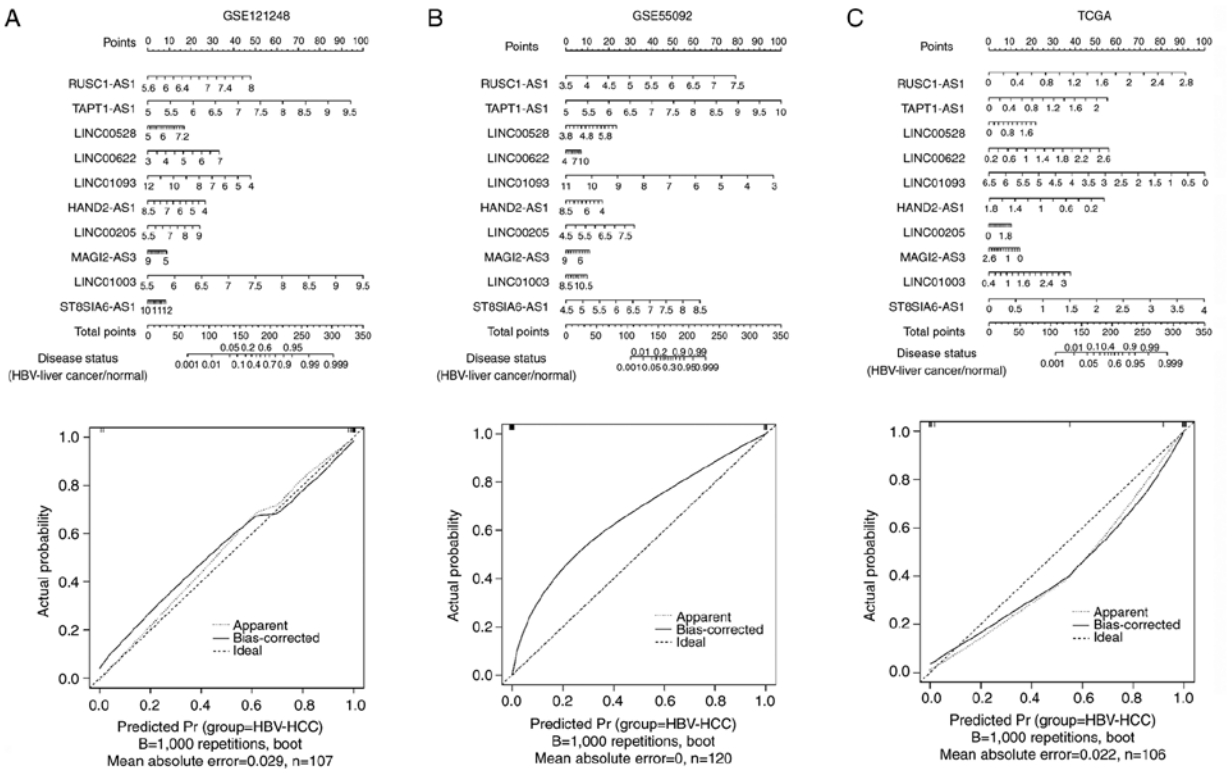

Figure 2. Nomogram construction. Nomogram models (upper) and calibration plots (lower) based on the 10-DElncRNA signature to predict the status of HBV-liver cancer in (A) GSE121248, (B) GSE55092 and (C) TCGA datasets. DElncRNA, differentially expressed long non-coding RNA; HBV, hepatitis B virus; TCGA, The Cancer Genome Atlas.

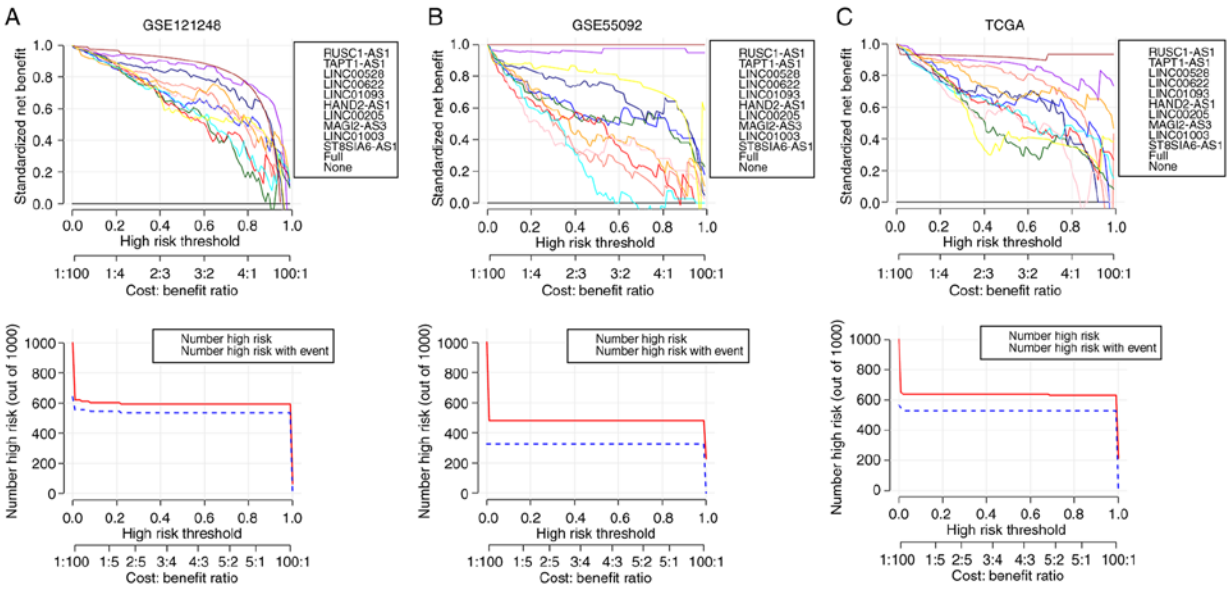

Figure 3. Validation of the nomogram. Decision curve analysis based on individual optimized lncRNA or combined optimized lncRNA signatures in (A) GSE121248, (B) GSE55092 and (C) TCGA datasets. lncRNA, long non-coding RNA; TCGA, The Cancer Genome Atlas.

Construction and validation of the nomogram. Using the 30 overlapping DElncRNAs, 13, 14 and 24 optimized lncRNA signatures were obtained using RFE, LASSO and RF algorithms, respectively (Fig. S2). After further screening, 10 optimized overlapping DElncRNAs were obtained, namely heart and neural crest derivatives expressed transcript 2 antisense RNA 1 (HAND2-AS1), LINC00622, ST8SIA6-AS1, TAPT1-AS1, MAGI2-AS3, LINC00528, LINC00205, RUSC1-AS1, LINC01093 and LINC01003. Next, a nomogram was constructed that integrated the 10-DElncRNA-based signature to predict the disease status of HBV-liver cancer in GSE121248 (Fig. 2A), GSE55092 (Fig. 2B) and TCGA (Fig. 2C) datasets. The corresponding calibration plots indicated that the nomogram had good accuracy as an ideal

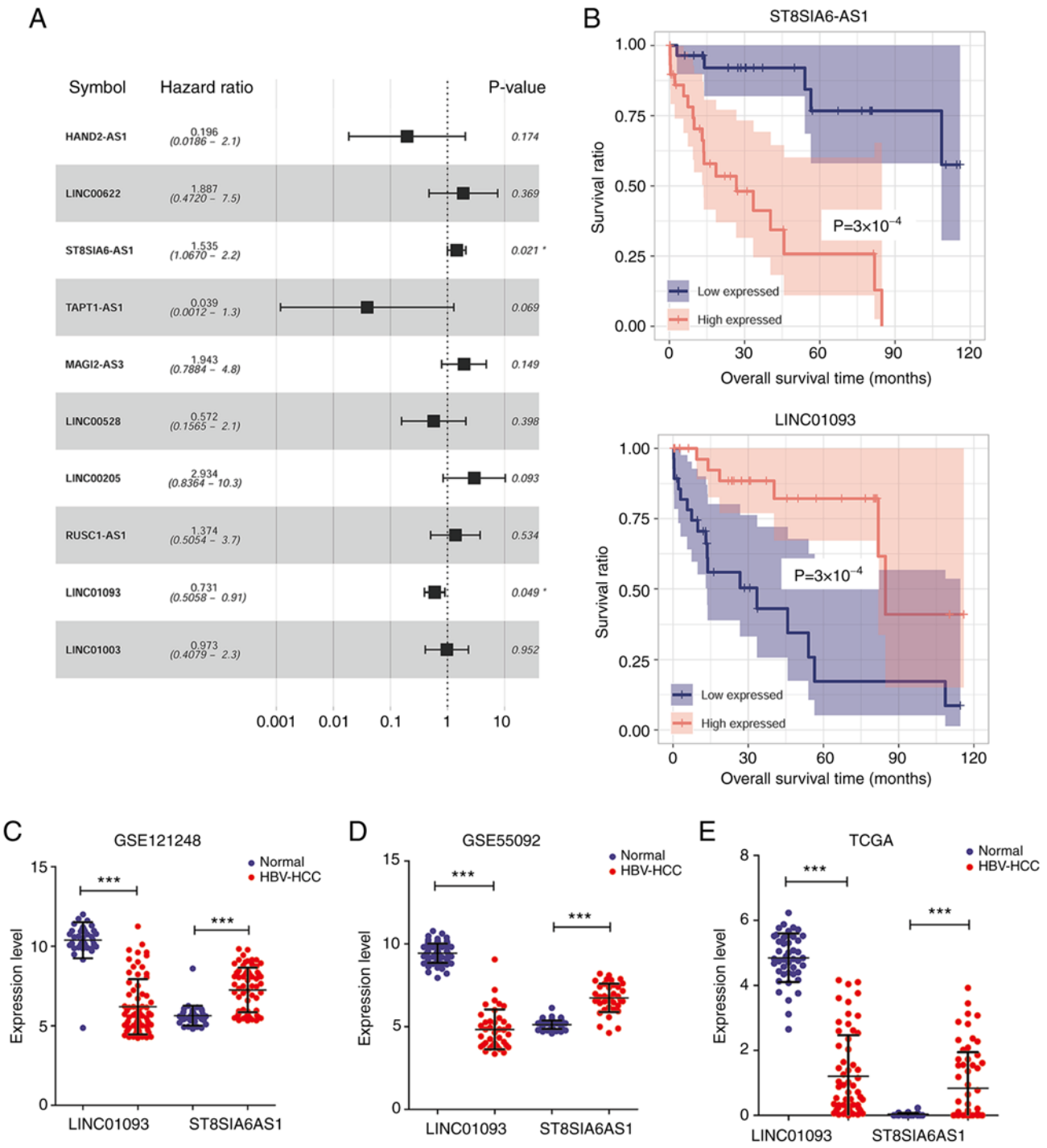

Figure 4. Prognostic performance of the HBV-associated lncRNA signature in liver cancer. (A) Forest plot for 10 prognosis-associated lncRNAs in HBV-liver cancer. (B) Kaplan-Meier survival analysis was performed to analyze the association of different expression levels of ST8SIA6-AS1 or LINC01093 with survival prognosis. The expression levels of ST8SIA6-AS1 and LINC01093 in HBV-liver cancer and normal tissues in (C) GSE121248, (D) GSE55092 and (E) TCGA datasets. ***P<0.001. HBV, hepatitis B virus; lncRNA, long non-coding RNA; TCGA, The Cancer Genome Atlas; HCC, hepatocellular carcinoma.

model for these three datasets. Moreover, the results from decision curve analysis showed the data from training dataset GSE121248 (Fig. 3A) were very consistent with the results in validation dataset GSE55092 (Fig. 3B) and independent validation dataset TCGA (Fig. 3C).

Prognostic performance of the HBV-related lncRNA signature in liver cancer. The survival prognosis information in TCGA dataset with univariate Cox regression analysis identified two lncRNAs that are associated with HBV-liver cancer prognosis, namely ST8SIA6-AS1 and LINC01093 with P<0.05, as displayed by forest plot (Fig. 4A). Kaplan-Meier survival analysis of TCGA dataset was performed to further assess the capability of these two lncRNAs to predict the prognosis of HBV-liver cancer. As shown in Fig. 4B, patients with HBV-liver cancer with downregulation of ST8SIA6-AS1 or upregulation of LINC01093 presented higher overall survival rates. As shown in Fig. 4C-E, ST8SIA6-AS1 was upregulated

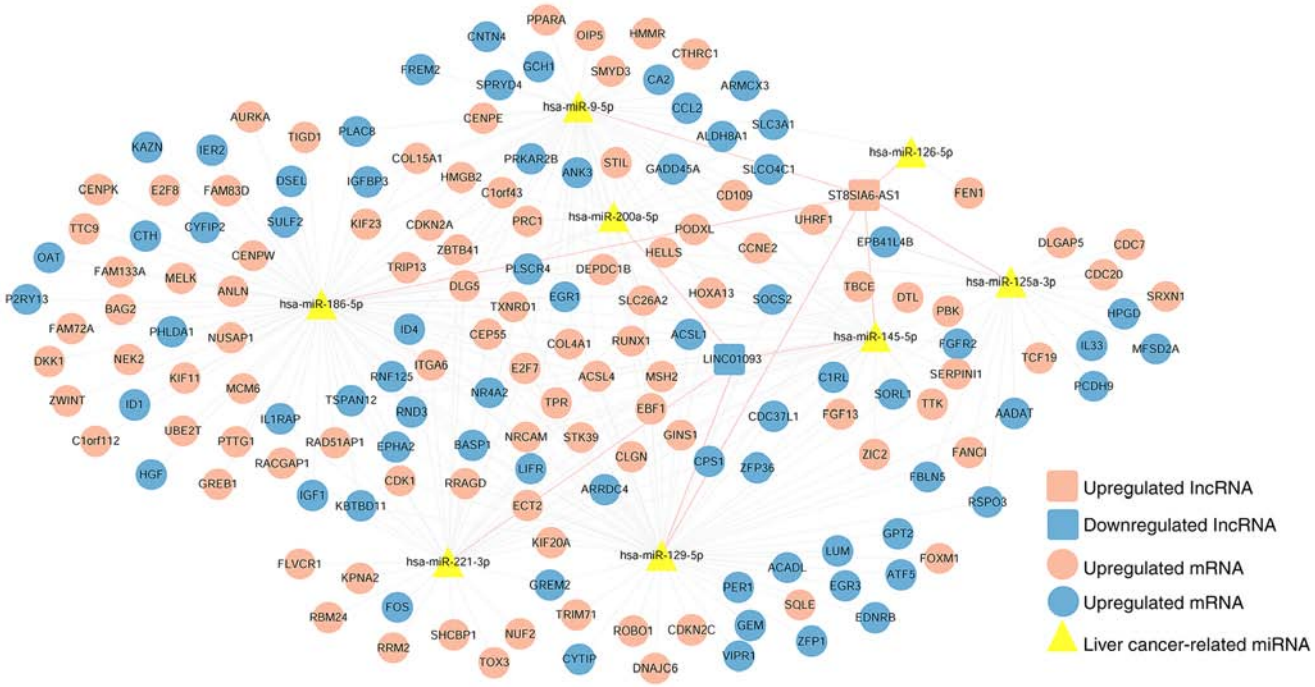

Figure 5. Construction of the competitive endogenous RNA network based on ST8SIA6-AS1 and LINC01093. Squares and circles represent DElncRNAs and regulated DEmRNAs, respectively. Red and blue represent significantly upregulated and downregulated expression factors, respectively, in HBV-liver cancer tumor samples. Yellow triangles represent liver cancer-associated miRNAs. The red and gray lines represent characteristic lncRNA-miRNA connections and miRNA-mRNA regulatory connections, respectively. DElncRNA, differentially expressed long non-coding RNA; DEmRNA, differentially expressed mRNA; HBV, hepatitis B virus; miRNA, microRNA.

while LINC01093 was downregulated in HBV-liver cancer samples compared with normal controls in the GSE121248, GSE55092 and TCGA datasets.

Construction of a ceRNA network based on the prognostic lncRNAs signature. Guided by the ceRNA hypothesis, 106 disease-associated miRNAs were identified, of which 77 miRNAs were associated with liver cancer (Table SIV). Using the DIANA-LncBasev2 database, the interactions of ST8SIA6-AS1 and LINC01093 with liver cancer-associated miRNAs were searched, and 11 highly linked lncRNA-miRNA interactions involving 8 liver cancer-associated miRNAs were obtained, which are shown in Table SV. The predicted mRNA targets of 8 liver cancer-associated miRNAs and 505 DEmRNAs were identified, and 285 miRNA-mRNA interactions were obtained (Table SVI). Finally, the ceRNA network was constructed; it comprised 172 interactions, and included 2 lncRNAs, 8 liver cancer-associated miRNAs and 162 DEmRNAs (Fig. 5). In addition, KEGG pathway enrichment analysis showed that the 162 DEmRNAs were significantly enriched in 8 KEGG signaling pathways (Fig. S3) and details of the pathways are displayed in Table I. By combining the DEmRNAs with the associated KEGG signaling pathways, a ceRNA regulatory network was constructed, as shown in Fig. 6.

Validation of selected lncRNA expression. To validate the accuracy of the data obtained by the bioinformatics analysis, the expression levels of ST8SIA6-AS1 and LINC01093 were measured using RT-qPCR in HBV-liver cancer samples collected from patients. The results showed that ST8SIA6-AS1 (Fig. 7A) was significantly upregulated, while LINC01093 (Fig. 7B) was significantly downregulated in the HBV-liver cancer tissues compared with the adjacent liver tissues. Consistent with this, the ST8SIA6-AS1 expression level was significantly upregulated in HepG2.2.15 cells compared with HepG2 cells (Fig. 7C), and the LINC01093 expression level was significantly downregulated in HepG2.2.15 cells when compared with HepG2 cells (Fig. 7D).

Investigation on the functional role of ST8SIA6-AS1 and LINC01093 in HBV-expressing liver cancer cells in vitro. The functional roles of ST8SIA6-AS1 and LINC01093 were investigated by performing loss-of-function and gain-of-function assays, respectively in HBV-expressing liver cancer cells. First, RT-qPCR confirmed the transfection efficiency of si-ST8SIA6-AS1 (Fig. 8A) and pcDNA3.1-LINC01093 (Fig. 8B) in HepG2.2.15 cells. In terms of HBV infection, the number of copies of HBV DNA in the supernatant of HepG2.2.15 cells was diminished after ST8SIA6-AS1 knockdown (Fig. 8C) or LINC01093 overexpression (Fig. 8D). ELISA results showed that the levels of viral factors HBsAg (Fig. 8E and F) and HBeAg (Fig. 8G and H) were significantly decreased in HepG2.2.15 cells after ST8SIA6-AS1 knockdown or LINC01093 overexpression. The ST8SIA6-AS1 downregulation and LINC01093 upregulation each lowered the HepG2.2.15 cell proliferation rate, as indicated by lower OD values after 72 h (Fig. 8I). In addition, the results of Transwell assays indicated that numbers of migrated and invaded cells were significantly reduced after ST8SIA6-AS1 knockdown (Fig. 8J) or LINC01093 overexpression (Fig. 8K) in HepG2.2.15 cells.

Table I. Significant KEGG pathways associated with differentially expressed mRNAs in the competitive endogenous RNA network.

KEGG terms	Count	P-value	Genes
hsa04110: Cell cycle	10	4.32×10^{-6}	CDC20, CDKN2C, PTTG1, CCNE2, CDKN2A, GADD45A, CDK1, TTK, CDC7, MCM6
hsa04115: p53 signaling pathway	7	8.62×10^{-5}	RRM2, CCNE2, CDKN2A, GADD45A, IGFBP3, CDK1, IGF1
hsa05200: Pathways in cancer	14	2.32×10^{-3}	CDKN2A, GADD45A, TXNRD1, HGF, FOS, IGF1, RUNX1, EDNRB, CCNE2, MSH2, COL4A1, TPR, ITGA6, FGFR2
hsa04114: Oocyte meiosis	6	1.01×10^{-2}	CDC20, PTTG1, CCNE2, CDK1, IGF1, AURKA
hsa03320: PPAR signaling pathway	4	3.96×10^{-2}	ACADL, ACSL1, ACSL4, PPARA
hsa04512: ECM-receptor interaction	4	4.59×10^{-2}	COL4A1, ITGA6, HMMR, FREM2
hsa00071: Fatty acid degradation	3	4.69×10^{-2}	ACADL, ACSL1, ACSL4
hsa04010: MAPK signaling pathway	7	4.75×10^{-2}	GADD45A, HGF, FOS, IL1RAP, IGF1, FGFR2, EPHA2

KEGG, Kyoto Encyclopedia of Genes and Genomes; PPAR, peroxisome proliferator-activated receptor; ECM, extracellular matrix.

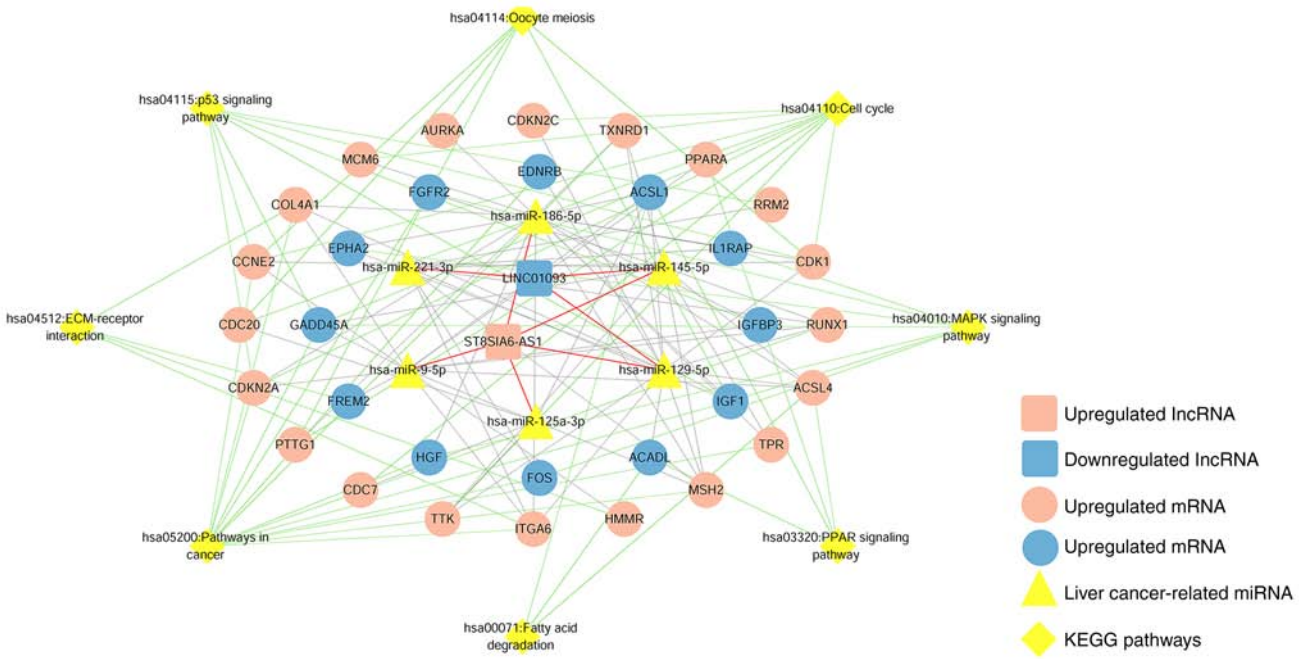

Figure 6. Construction of the competitive endogenous RNA network based on DEmRNA in KEGG pathways. Squares and circles represent DElncRNAs and regulated DEmRNAs, respectively. Red and blue represent significantly upregulated and downregulated expression factors, respectively, in HBV-liver cancer tumor samples. Yellow triangles represent liver cancer-associated miRNAs. The red and gray lines represent characteristic lncRNA-miRNA connections and miRNA-mRNA regulatory connections, respectively. Rhombuses represent KEGG pathways with green connections. DEmRNA, differentially expressed mRNA; DElncRNA, differentially expressed long non-coding RNA; miRNA, microRNA; Kyoto Encyclopedia of Genes and Genomes.

Discussion

To the best of current knowledge, persistent HBV infection is the leading cause of liver cancer (32), which is considered to promote the initiation and progression of liver cancer by integrating into the host genome (33). Numerous studies have elucidated the crucial role of lncRNAs in HBV-associated liver cancer (34). In the present study, three gene expression datasets were analyzed, in which 30 DElncRNAs and 505 DEmRNAs were identified in HBV-associated liver cancer samples compared with controls. GO and KEGG enrichment analyses demonstrated these DEmRNAs were associated with various metabolic processes, 'extracellular region', 'oxidoreductase activity', 'cell cycle' and 'PPAR signaling pathway'. Cancer is clearly associated with abnormal metabolic processes, and enzymes that contribute to altered retinol metabolism have been shown to participate in the development of liver cancer (35). Cell cycle deregulation is associated with the initiation of cancer through the mutation of proteins with key roles at different stages of the cell cycle (36). Previous studies have shown that peroxisome proliferator-activated receptors (PPARs) are nuclear receptors that function as transcription

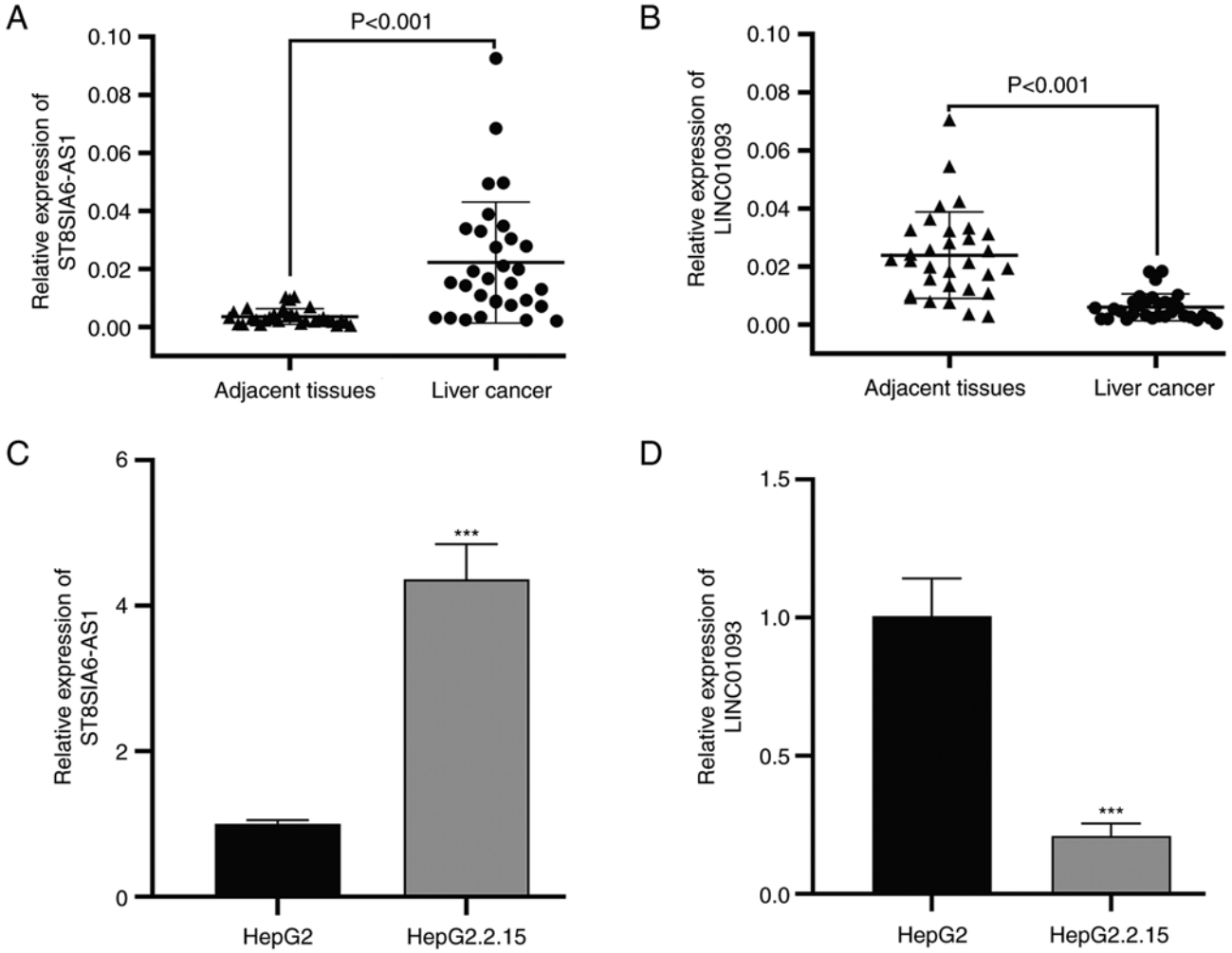

Figure 7. Expression of ST8SIA6-AS1 and LINC01093 in liver cancer tissues and cells. RT-qPCR was used to determine the expression levels of (A) ST8SIA6-AS1 and (B) LINC01093 in hepatitis B-associated liver cancer samples and adjacent liver tissues (n=31). The expression levels of ST8SIA6-AS1 and LINC01093 were also measured by RT-qPCR in (C) HepG2 and (D) HepG2.2.15 cells. ***P<0.001 vs. HepG2. Data are presented as the mean ± SD of three independent experiments. RT-qPCR, reverse transcription-quantitative PCR.

factors and regulate physiological activities including invasion, immune tolerance, metabolism and inflammation (37,38). For example, a study revealed that the activation of PPAR-α was involved in the tumor-promoting effects of 4-phenylbutyric acid in a liver cancer-inducing environment (39).

Feature selection along with three optimization algorithms were employed to identify 10 optimal DElncRNA-based signatures consisting of HAND2-AS1, LINC00622, ST8SIA6-AS1, TAPT1-AS1, MAGI2-AS3, LINC00528, LINC00205, RUSC1-AS1, LINC01093 and LINC01003. HAND2-AS1 has been reported to be required for the self-renewal maintenance of liver cancer stem cells to initiate liver cancer development (40). Furthermore, HAND2-AS1 overexpression has been shown to inhibit cancer cell proliferation in liver cancer via the downregulation of runt-related transcription factor 2 expression (41). ST8SIA6-AS1 has been reported to be a cancer-associated lncRNA that facilitates cell proliferation and resistance to apoptosis in liver cancer cells (42). Consistent with this, Zhang *et al* (43) demonstrated that the downregulation of ST8SIA6-AS1 suppressed liver cancer cell proliferation, migration and invasion *in vitro* and restrained liver cancer tumorigenesis *in vivo*. MAGI2-AS3 has been found to be downregulated in the plasma of patients with early-stage liver cancer, while the overexpression of MAGI2-AS3 exerts suppressive effects on the proliferation and migration of liver cancer cells (44-46). LINC00205, a bidirectional lncRNA, located at human chromosome 21q22.3, has been characterized as an oncogenic molecule that contributes to cell proliferation in liver cancer (47,48). Liu *et al* (49) recently reported that the knockdown of RUSC1-AS1 inhibited liver cancer cell progression, including proliferation, migration and invasion, and suppressed tumorigenesis *in vivo*. LINC01093, as a recently identified liver-specific lncRNA, has been shown to suppress liver cancer cell proliferation and metastasis *in vitro* and *in vivo* (50). However, studies on the involvement of HAND2-AS1, TAPT1-AS1, LINC00528 and LINC01003 in liver cancer are lacking.

Based on the survival prognosis information in TCGA dataset, ST8SIA6-AS1 and LINC01093 were further screened as HBV-liver cancer prognosis-associated lncRNAs. Patients whose HBV-liver cancer had low ST8SIA6-AS1 or high LINC01093 expression levels had an improved overall survival rate. *In vitro* experiments confirmed that ST8SIA6-AS1 was upregulated in HBV-expressing liver cancer cells, and

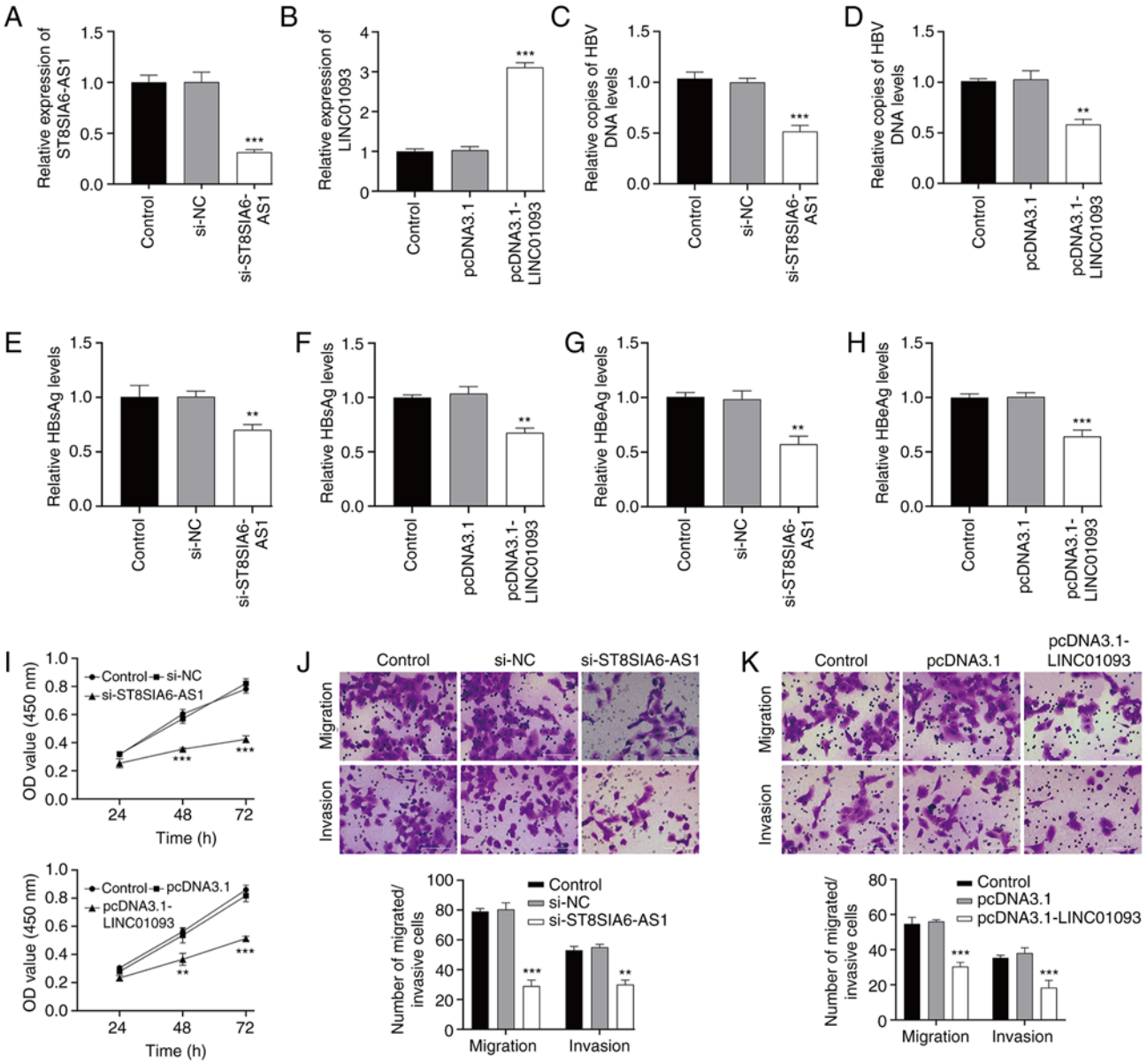

Figure 8. Investigation of the functional role of ST8SIA6-AS1 and LINC01093 in HBV-expressing liver cancer cells *in vitro*. HepG2.2.15 cells were transfected with si-ST8SIA6-AS1 and si-NC or pcDNA3.1-LINC01093 and pcDNA3.1, respectively. RT-qPCR was used to determine the expression levels of (A) ST8SIA6-AS1 and (B) LINC01093 in transfected HepG2.2.15 cells. (C and D) qPCR detected copies of HBV DNA in culture supernatants of the transfected HepG2.2.15 cells. ELISAs were used to measure levels of viral factors in the cell culture supernatants; specifically, HBsAg in (E) ST8SIA6-AS1 knockdown and (F) LINC01093 overexpressing cells, and HBeAg in (G) ST8SIA6-AS1 knockdown and (H) LINC01093 overexpressing cells. (I) Cell Counting Kit-8 assay was used to evaluate OD value of the transfected HepG2.2.15 cells at 450 nm. Transwell assays were used to determine the numbers of migrated and invaded cells in the (J) ST8SIA6-AS1 knockdown and (K) LINC01093 overexpressing cells. Data are presented as the mean ± SD. **P<0.01, ***P<0.001 vs. si-NC or pcDNA3.1. HBV, hepatitis B virus; si, small interfering; NC, negative control; RT-qPCR, reverse transcription-quantitative PCR; HBsAg, hepatitis B surface antigen; HBeAg, hepatitis B e antigen; OD, optical density.

the knockdown of ST8SIA6-AS1 in these cells significantly suppressed cell proliferation, migration and invasion, as well as HBV expression and replication. Consistent with these data, Qin *et al* (51) revealed that the upregulation of ST8SIA6-AS1 is associated with higher tumor stages and metastasis, and thus has potential as a diagnostic biomarker for liver cancer progression. Although the role of ST8SIA6-AS1 in HBV-liver cancer cells has not been reported previously, to the best of our knowledge, the promotive effects of ST8SIA6-AS1 on cell proliferation, migration and invasion have already been elucidated in liver cancer cells (52,53). Consistent with the present data showing that LINC01093 was downregulated in HBV-expressing liver cancer cells and suppressed proliferation and mobility, Mou *et al* (54) identified LINC01093 as an optimal diagnostic and prognostic lncRNA biomarker for HBV-associated liver cancer. The previously reported suppressive effects of LINC01093 on liver cancer cell proliferation and metastasis (50) support the finding that LINC01093 acts a tumor suppressor in HBV-liver cancer cells. Furthermore, the ceRNA network based on ST8SIA6-AS1 and LINC01093 was constructed in the present study, which included 8 liver cancer-miRNAs and 162 DEmRNAs.

The present study has some limitations as follows: i) Large HBV-liver cancer cohorts are required to confirm

the prognostic values of the lncRNA signature; ii) further wet experiments are necessary to verify the mechanisms indicated by the ceRNA network, for example luciferase assays with overexpression or silencing, or co-expression (coimmunoprecipitation); iii) *in vivo* experiments are essential to validate the functional role of ST8SIA6-AS1 and LINC01093; iv) further mechanistic analysis is required to confirm the oncogenic or suppressive roles of these two lncRNAs.

In summary, 10 optimal DElncRNA-based signatures of HBV-associated liver cancer were constructed based on microarray datasets, which created a nomogram with good accuracy as an ideal model. ST8SIA6-AS1 and LINC01093 were further identified as lncRNAs that are associated with HBV-liver cancer prognosis and further analyses demonstrated that they may play important roles in the progression of HBV-liver cancer. Collectively, these data may provide an understanding of the regulatory mechanisms of lncRNAs in the development of HBV-associated liver cancer and help the identification of potential targets for its treatment.

Acknowledgements

Not applicable.

Funding

This study was supported by the Cultivation of Academic Leaders in Pudong New Area (grant no. PWRd2021-20) and Shanghai Traditional Chinese Medicine Capacity Building Project for the Prevention and Treatment of Infectious Diseases (grant no. ZYYB-NLPY-04).

Availability of data and materials

The datasets used and/or analyzed during the current study are available from the corresponding author on reasonable request.

Authors' contributions

XW conceived the design of the study. JX and HZ acquired the data and conducted the statistical analysis. YF collected tissue samples and participated in the interpretation of the data. XL and XW analyzed and interpreted the data, and drafted and revised the manuscript. All authors read and approved the final manuscript. XW and JX confirm the authenticity of all the raw data.

Ethics approval and consent to participate

All human tissues were obtained in accordance with the Declaration of Helsinki (1975) and approved by the Ethics Committee of Hospital for Infectious Diseases of Pudong District (Shanghai, China; approval no. IDP-2020PD; 2020.8.16). Each patient provided written informed consent for the use of their samples in scientific research.

Patient consent for publication

Not applicable.

Competing interests

The authors declare that they have no competing interests.

References

1. Erratum: Global cancer statistics 2018: GLOBOCAN estimates of incidence and mortality worldwide for 36 cancers in 185 countries. CA Cancer J Clin 70: 313, 2020.
2. Yang F, Ma L, Yang Y, Liu W, Zhao J, Chen X, Wang M, Zhang H, Cheng S, Shen F, *et al*: Contribution of hepatitis B virus infection to the aggressiveness of primary liver cancer: A clinical epidemiological study in Eastern China. Front Oncol 9: 370, 2019.
3. Liu YC, Lu LF, Li CJ, Sun NK, Guo JY, Huang YH, Yeh CT and Chao CCK: Hepatitis B virus X protein induces RHAMM-dependent motility in hepatocellular carcinoma cells via PI3K-Akt-Oct-1 signaling. Mol Cancer Res 18: 375-389, 2020.
4. Kang I, Kim JA, Kim J, Lee JH, Kim MJ and Ahn JK: Hepatitis B virus X protein promotes epithelial-mesenchymal transition of hepatocellular carcinoma cells by regulating SOCS1. BMB Rep 55: 220-225, 2022.
5. Lei Y, Xu X, Liu H, Chen L, Zhou H, Jiang J, Yang Y and Wu B: HBx induces hepatocellular carcinogenesis through ARRB1-mediated autophagy to drive the G(1)/S cycle. Autophagy 17: 4423-4441, 2021.
6. European Association for the Study of the Liver. Electronic address: easloffice@easloffice.eu; European Association for the Study of the Liver: EASL clinical practice guidelines: Management of hepatocellular carcinoma. J Hepatol 69: 182-236, 2018.
7. Li LM, Chen C, Ran RX, Huang JT, Sun HL, Zeng C, Zhang Z, Zhang W and Liu SM: Loss of TARBP2 drives the progression of hepatocellular carcinoma via miR-145-SERPINE1 axis. Front Oncol 11: 620912, 2021.
8. Qiu L, Wang T, Xu X, Wu Y, Tang Q and Chen K: Long non-coding RNAs in hepatitis B virus-related hepatocellular carcinoma: Regulation, functions, and underlying mechanisms. Int J Mol Sci 18: 2505, 2017.
9. Fortes P and Morris KV: Long noncoding RNAs in viral infections. Virus Res 212: 1-11, 2016.
10. Stojic L, Lun ATL, Mascalchi P, Ernst C, Redmond AM, Mangei J, Barr AR, Bousgouni V, Bakal C, Marioni JC, *et al*: A high-content RNAi screen reveals multiple roles for long noncoding RNAs in cell division. Nat Commun 11: 1851, 2020.
11. Hou Z, Xu X, Fu X, Tao S, Zhou J, Liu S and Tan D: HBx-related long non-coding RNA MALAT1 promotes cell metastasis via up-regulating LTBP3 in hepatocellular carcinoma. Am J Cancer Res 7: 845-856, 2017.
12. Tao L, Li D, Mu S, Tian G and Yan G: LncRNA MAPKAPK5_AS1 facilitates cell proliferation in hepatitis B virus-related hepatocellular carcinoma. Lab Invest 102: 494-504, 2022.
13. Deng Y, Wei Z, Huang M, Xu G, Wei W, Peng B, Nong S and Qin H: Long non-coding RNA F11-AS1 inhibits HBV-related hepatocellular carcinoma progression by regulating NR1I3 via binding to microRNA-211-5p. J Cell Mol Med 24: 1848-1865, 2020.
14. Huang JL, Ren TY, Cao SW, Zheng SH, Hu XM, Hu YW, Lin L, Chen J, Zheng L and Wang Q: HBx-related long non-coding RNA DBH-AS1 promotes cell proliferation and survival by activating MAPK signaling in hepatocellular carcinoma. Oncotarget 6: 33791-33804, 2015.
15. Zhang H, Diab A, Fan H, Mani SKK, Hullinger R, Merle P and Andrisani O: PLK1 and HOTAIR accelerate proteasomal degradation of SUZ12 and ZNF198 during hepatitis B virus-induced liver carcinogenesis. Cancer Res 75: 2363-2374, 2015.
16. Wang J, Yin G, Bian H, Yang J, Zhou P, Yan K, Liu C, Chen P, Zhu J, Li Z and Xue T: LncRNA XIST upregulates TRIM25 via negatively regulating miR-192 in hepatitis B virus-related hepatocellular carcinoma. Mol Med 27: 41, 2021.
17. Liu H, Zhao P, Jin X, Zhao Y, Chen Y, Yan T, Wang J, Wu L and Sun Y: A 9lncRNA risk score system for predicting the prognosis of patients with hepatitis B viruspositive hepatocellular carcinoma. Mol Med Rep 20: 573-583, 2019.
18. Wang SM, Ooi LL and Hui KM: Identification and validation of a novel gene signature associated with the recurrence of human hepatocellular carcinoma. Clin Cancer Res 13: 6275-6283, 2007.

19. Melis M, Diaz G, Kleiner DE, Zamboni F, Kabat J, Lai J, Mogavero G, Tice A, Engle RE, Becker S, *et al*: Viral expression and molecular profiling in liver tissue versus microdissected hepatocytes in hepatitis B virus-associated hepatocellular carcinoma. J Transl Med 12: 230, 2014.
20. Ritchie ME, Phipson B, Wu D, Hu Y, Law CW, Shi W and Smyth GK: limma powers differential expression analyses for RNA-sequencing and microarray studies. Nucleic Acids Res 43: e47, 2015.
21. Huang DW, Sherman BT and Lempicki RA: Systematic and integrative analysis of large gene lists using DAVID bioinformatics resources. Nat Protocols 4: 44-57, 2009.
22. Huang DW, Sherman BT and Lempicki RA: Bioinformatics enrichment tools: Paths toward the comprehensive functional analysis of large gene lists. Nucleic Acids Res 37: 1-13, 2009.
23. Deist TM, Dankers F, Valdes G, Wijsman R, Hsu IC, Oberije C, Lustberg T, van Soest J, Hoebers F, Jochems A, *et al*: Machine learning algorithms for outcome prediction in (chemo) radiotherapy: An empirical comparison of classifiers. Med Phys 45: 3449-3459, 2018.
24. Goeman JJ: L1 penalized estimation in the Cox proportional hazards model. Biom J 52: 70-84, 2010.
25. Tolosi L and Lengauer T: Classification with correlated features: Unreliability of feature ranking and solutions. Bioinformatics 27: 1986-1994, 2011.
26. Wu J, Zhang H, Li L, Hu M, Chen L, Xu B and Song Q: A nomogram for predicting overall survival in patients with low-grade endometrial stromal sarcoma: A population-based analysis. Cancer Commun (Lond) 40: 301-312, 2020.
27. Jiang Q, Wang Y, Hao Y, Juan L, Teng M, Zhang X, Li M, Wang G and Liu Y: miR2Disease: A manually curated database for microRNA deregulation in human disease. Nucleic Acids Res 37: D98-D104, 2009.
28. Paraskevopoulou MD, Vlachos IS, Karagkouni D, Georgakilas G, Kanellos I, Vergoulis T, Zagganas K, Tsanakas P, Floros E, Dalamagas T and Hatzigeorgiou AG: DIANA-LncBase v2: Indexing microRNA targets on non-coding transcripts. Nucleic Acids Res 44: D231-D238, 2016.
29. Li JH, Liu S, Zhou H, Qu LH and Yang JH: starBase v2.0: Decoding miRNA-ceRNA, miRNA-ncRNA and protein-RNA interaction networks from large-scale CLIP-Seq data. Nucleic Acids Res 42: D92-D97, 2014.
30. Shannon P, Markiel A, Ozier O, Baliga NS, Wang JT, Ramage D, Amin N, Schwikowski B and Ideker T: Cytoscape: A software environment for integrated models of biomolecular interaction networks. Genome Res 13: 2498-2504, 2003.
31. Livak KJ and Schmittgen TD: Analysis of relative gene expression data using real-time quantitative PCR and the 2(-Delta Delta C(T)) method. Methods 25: 402-408, 2001.
32. Ridruejo E: Does hepatitis B virus therapy reduce the risk of hepatocellular carcinoma? Expert Opin Drug Saf 14: 439-451, 2015.
33. Bisceglie AMD: Hepatitis B and hepatocellular carcinoma. Hepatology 49: S56-S60, 2009.
34. Chauhan R and Lahiri N: Tissue- and serum-associated biomarkers of hepatocellular carcinoma. Biomarkers Cancer 8: 37-55, 2016.
35. Pettinelli P, Arendt BM, Teterina A, McGilvray I, Comelli EM, Fung SK, Fischer SE and Allard JP: Altered hepatic genes related to retinol metabolism and plasma retinol in patients with non-alcoholic fatty liver disease. PLoS One 13: e0205747, 2018.
36. Liping X, Jia L, Qi C, Liang Y, Dongen L and Jianshuai J: Cell Cycle Genes are potential diagnostic and prognostic biomarkers in hepatocellular carcinoma. Biomed Res Int 2020: 6206157, 2020.
37. Lee CH, Olson P and Evans RM: Minireview: Lipid metabolism, metabolic diseases, and peroxisome proliferator-activated receptors. Endocrinology 144: 2201-2207, 2003.
38. Oyefiade A, Erdman L, Goldenberg A, Malkin D, Bouffet E, Taylor MD, Ramaswamy V, Scantlebury N and Law N: PPAR and GST polymorphisms may predict changes in intellectual functioning in medulloblastoma survivors. J Neurooncol 142: 39-48, 2019.
39. Chen SZ, Ling Y, Yu LX, Song YT, Chen XF, Cao QQ, Yu H, Chen C, Tang JJ, Fan ZC, *et al*: 4-phenylbutyric acid promotes hepatocellular carcinoma via initiating cancer stem cells through activation of PPAR-α. Clin Transl Med 11: e379, 2021.
40. Wang Y, Zhu P, Luo J, Wang J, Liu Z, Wu W, Du Y, Ye B, Wang D, He L, *et al*: LncRNA HAND2-AS1 promotes liver cancer stem cell self-renewal via BMP signaling. EMBO J 38: e101110, 2019.
41. Jing GY, Zheng XZ and Ji XX: lncRNA HAND2-AS1 overexpression inhibits cancer cell proliferation in hepatocellular carcinoma by downregulating RUNX2 expression. J Clin Lab Anal 35: e23717, 2021.
42. Fei Q, Song F, Jiang X, Hong H, Xu X, Jin Z, Zhu X, Dai B, Yang J, Sui C and Xu M: LncRNA ST8SIA6-AS1 promotes hepatocellular carcinoma cell proliferation and resistance to apoptosis by targeting miR-4656/HDAC11 axis. Cancer Cell Int 20: 232, 2020.
43. Zhang X, Xu S, Hu C, Fang K, Zhou J, Guo Z, Zhu G and Li L: LncRNA ST8SIA6-AS1 promotes hepatocellular carcinoma progression by regulating MAGEA3 and DCAF4L2 expression. Biochem Biophys Res Commun 533: 1039-1047, 2020.
44. Yin Z, Ma T, Yan J, Shi N, Zhang C, Lu X, Hou B and Jian Z: LncRNA MAGI2-AS3 inhibits hepatocellular carcinoma cell proliferation and migration by targeting the miR-374b-5p/SMG1 signaling pathway. J Cell Physiol 234: 18825-18836, 2019.
45. Fang G, Wang J, Sun X, Xu R, Zhao X, Shao L, Sun C and Wang Y: LncRNA MAGI2-AS3 is downregulated in the distant recurrence of hepatocellular carcinoma after surgical resection and affects migration and invasion via ROCK2. Ann Hepatol 19: 535-540, 2020.
46. Wei H, Tang Q, Wang A, Zhang Y, Qin Z, Li W, Xu Z, Wang J and Pu J: lncRNA MAGI2-AS3 exerts antioncogenic roles in hepatocellular carcinoma via regulating the miR-519c-3p/TXNIP Axis. J Oncol 2021: 5547345, 2021.
47. Zhang L, Wang Y, Sun J, Ma H and Guo C: LINC00205 promotes proliferation, migration and invasion of HCC cells by targeting miR-122-5p. Pathol Res Pract 215: 152515, 2019.
48. Cheng T, Yao Y, Zhang S, Zhang XN, Zhang AH, Yang W and Hou CZ: LINC00205, a YY1-modulated lncRNA, serves as a sponge for miR-26a-5p facilitating the proliferation of hepatocellular carcinoma cells by elevating CDK6. Eur Rev Med Pharmacol Sci 25: 6208-6219, 2021.
49. Liu C, Tang L, Xu M, Lin Y, Shen J, Zhou L, Ho L, Lu J and Ai X: LncRNA RUSC1-AS1 contributes to the progression of hepatocellular carcinoma cells by modulating miR-340-5p/CREB1 axis. Am J Transl Res 13: 1022-1036, 2021.
50. He J, Zuo Q, Hu B, Jin H, Wang C, Cheng Z, Deng X, Yang C, Ruan H, Yu C, *et al*: A novel, liver-specific long noncoding RNA LINC01093 suppresses HCC progression by interaction with IGF2BP1 to facilitate decay of GLI1 mRNA. Cancer Lett 450: 98-109, 2019.
51. Qin SJ, Zhou HZ, Xu NS, Yang HC and Chen PX: The diagnostic value of serum ST8SIA6-AS1 as biomarker in hepatocellular carcinoma. Clin Lab 66: doi: 10.7754/Clin.Lab.2020.200231, 2020.
52. Kuai J, Zheng L, Yi X, Liu Z, Qiu B, Lu Z and Jiang Y: ST8SIA6-AS1 promotes the development of hepatocellular carcinoma cells through miR-338-3p/NONO axis. Digestive Liver Dis 53: 1192-1200, 2021.
53. Zhang B, Liu Z, Liu J, Cao K, Shan W, Wen Q and Wang R: Long non-coding RNA ST8SIA6-AS1 promotes the migration and invasion of hypoxia-treated hepatocellular carcinoma cells through the miR-338/MEPCE axis. Oncol Rep 45: 73-82, 2021.
54. Mou Y, Wang D, Xing R, Nie H, Mou Y, Zhang Y and Zhou X: Identification of long noncoding RNAs biomarkers in patients with hepatitis B virus-associated hepatocellular carcinoma. Cancer Biomark 23: 95-106, 2018.